A Background ATR transmission spectra

Changes of amplitudes $A_{x,y}$ due to absorption in the sample and phase angle changes $\psi_{x,y}$ due to refractive index contrast n_2/n_1 can be accounted for by using fixed polarisation for the excitation (IN-port) and carrying polarisation analysis at the OUT-port. Such analysis carried out for each spectral point of hyperspectral data reveals absorbance and retardance (phase) related changes over the measured spectral range (no K-K modeling is required).

Even for a reference measurement of ATR setup (air instead of sample), the data measured at four different input polarisations showed complex fits in terms of amplitudes A and phase angles ψ (Fig. 2(a)). Interestingly, the polar dependence of ATR transmission becomes simpler when plotted against the relative angle $(\theta_{out} - \theta_{in})$ as shown in Fig. 2(b). Such angular dependence is similar to the case when an optical retarder is inserted between two polarisers (cross Nicol measurement), i.e., an overall transmittance is maximum when polariser and analyser are aligned for maximum transmission $(\theta_{out} - \theta_{in} = 0)$ and minimum when crossed $(\pi/2)$. This presentation was adapted for analysis of all hyperspectral data set at each wavenumber.

Transmittance through the ATR setup without sample (air) is shown in Fig. S1. Note that when $\Delta A \to 0$ phase become undefined (b). Two terms of Eq. 1 the in-phase and out-of-phase had different weight as shown in (a); the horizontal in-plane x-component corresponds to the major portion of synchrotron THz-IR radiation. The phase (b) was constant over the all spectral region and was around $\Delta\psi = 0$ rad for the x- and y-components defined at the IN-port (Polariser-2). Such transmission anisotropy ΔA and $\Delta\phi$ corresponds to an optical retarder (the ATR unit) with slow(or fast) axis parallel or perpendicular to the H (0) or V $(\pi/2)$ orientations at the entrance of IN-port (synchrotron THz-IR radiation has strongest component along X). The x and y-components showed anti-correlation trend, which is consistent with Fresnel reflection at $\theta_i \neq 0^\circ$ (not normal incidence) conditions when s- and p-polarisations are interchanged when traversing ten reflections in the ATR unit. Phase difference $\Delta\psi$ for $\pm\pi/4$ components selected at the IN-port showed smaller phase variations within a band of 3° phase difference (Fig. S1(b)). A consistent 3° separation between $\pm\pi/4$ polarisations is caused by off-axis incidence of THz beam onto ATR prism (by ATR design). This phase relation is a consequence of commutative phase changes occurring on the multi-reflections encountered in ATR unit. The phase changes at the ATR prism - air (or sample) interface are well defined and can be calculated for the known refractive index constant and irradiation angle (see Appendix of the reference [12]).

B Transmittance of ATR unit and Absorbance in PLLA

Figure S3 shows differential transmittance spectra for four different orientations of the incidence beam (at IN-port) in (a). The panel (b) is a differential retardance spectra at the same spectral window. Similar tendencies as for the PHB spectra (Fig. 3) are discernible. Strong phase changes between x- and y-phases $\Delta\phi$ occur at the position of absorption bands (Fig. 4). It is fully consistent with phase change around the absorption band (Lorenzian resonance) shown in Fig. 5.

C Four-polarisation Transmittance in ATR

The 4-angle polarisation method used to determine orientation of absorbers θ_A from a far-field transmittance, was applied for the non-propagating near-fields. Equation 1 establishes the base for the analysis. The absorbers follow a $\cos^2(\theta - \theta_A)$ orientation dependence, i.e., absorber has the maximum absorbance (minimum in transmittance T) after π rotation. The 4-angle polarisation method can be applied when polarisaiton at the IN-port is fixed to one of the angles $\theta = 0, \pi/4, \pi/2, 3\pi/4$, and all polarisations are summed at the OUT-port. This corresponds to an integration of Eq. 1 from 0 to 2π; the integrals $\int \cos^2\theta d\theta = \frac{\theta}{2} + \frac{\sin(2\theta)}{4} + Const$ and $\int \sin^2\theta d\theta = \frac{\theta}{2} - \frac{\sin(2\theta)}{4} + Const$. We adopted the approach of adding of two x- and y-components (s- and p-polarisations) of T at the OUT-port and $\int_0^{2\pi}(T_x\cos^2\theta + T_y\sin^2\theta)d\theta = \pi(T_x + T_y)$, which is appropriate to construct polarisation independent transmittance from the two orthogonal components [36].

The bottom of Fig. S4 shows 4-angle polarisation data (markers) and absorbance band fits by $\propto \cos^2\theta$, which probe out-of-plane in the xy plane (Fig. 5(b)) - orientation of absorbance. This dependence is expected for the absorbing dipole and validates the proposed method. There is an increasing number of applications where absorption in nano-thin films can be very important due to the optical near-field coupling of metal-insulator-metal (MIM) metamaterials. Such coupling takes place in the nano-cavity between metal back-mirror and nano-particle of MIM and is typically perpendicular to the incident/reflected light onto the MIM pattern, hence, it is out-of-plane to the sample's surface. It was shown recently, that such coupling is critically important for creation of perfect absorbers [37], where scattering losses should exactly match those of absorption (at the point of zero refection). This study of the ATR polariscopy/tomography shows how to harness optical near-fields and to probe optical properties of materials along the direction of light propagation. Near-field polariscopy could be widely used in metamaterials and topological photonics.

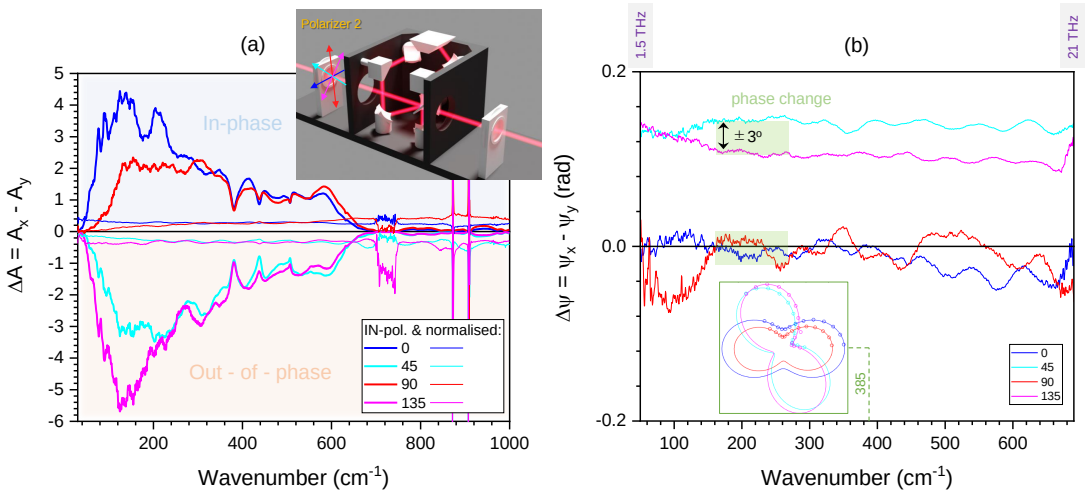

Fig. S1 ATR transmittance spectra of air (no sample) plotted as the difference in absorbance amplitude $\Delta A = A_x - A_y$ (a) and retardance phase $\Delta\psi = \psi_x - \psi_y$ (b) calculated from the best fit by Eq. 1; 0.26 rad $\approx \pi/12 = 15°$. The normalised $\Delta A/\tilde{S}$ are plotted by thin lines (see Fig. S2 for $\tilde{S}$ spectrum). The inset in (a) shows color conventions for input polarisation; inset in (b) shows the specific xy-intensity map (same as in Fig. 2(b)). See Fig. S2 for the reference spectra: transmission of synchrotron THz radiation through the entire ATR setup.

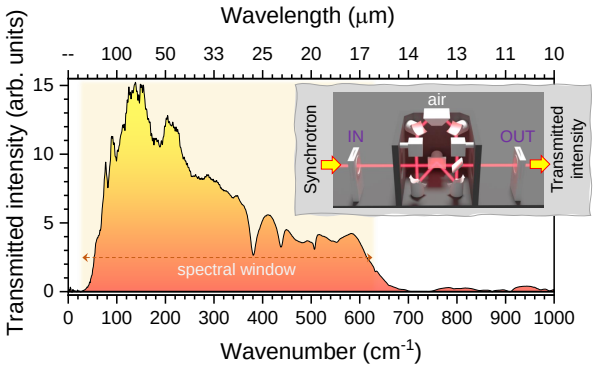

Fig. S2 Measured reference ATR transmission spectra $\tilde{S}$ calculated as a sum of four polariser-analyser angular settings at the IN- and OUT-ports (IN,OUT): $\tilde{S} = HH + HV + VV + VH \equiv (0,0) + (0,\pi/2) + (\pi/2,\pi/2) + (\pi/2,0)$. The wavenumber (bottom) $\tilde{\nu} = 1/\lambda$ and wavelength (top) axes are shown for reference $\tilde{\nu}$ [cm^{-1}] $\equiv 10^4/\lambda$ [μm]. The spectral window of 30-630 cm^{-1} (shaded region) was selected with beamsplitter and the detector (Si bolometer). Inset shows IN-/OUT-ports where polarisers were set at the entrance and exit positions of the ATR unit.

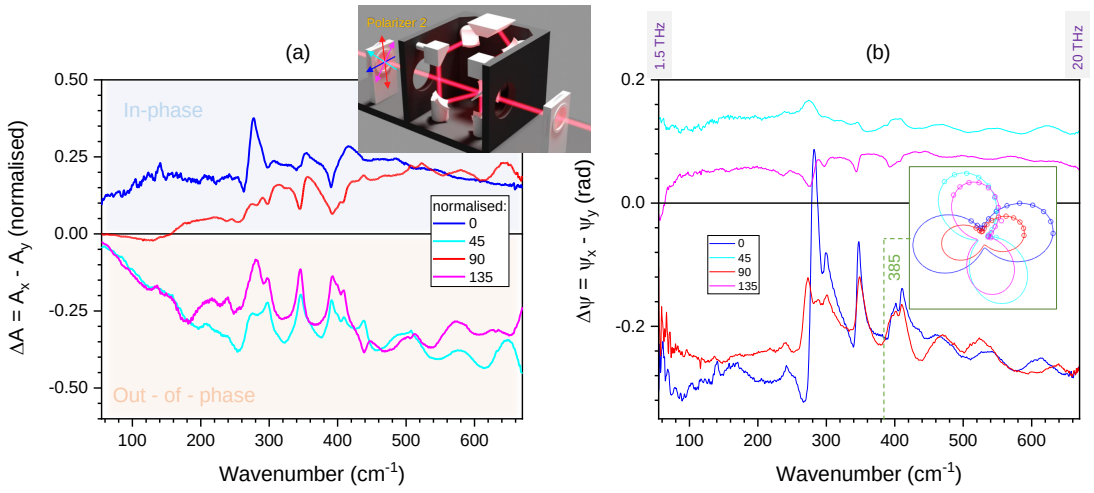

Fig. S3 ATR transmittance spectra of poly-l-lacic acid (PLLA) plotted as the difference in absorbance amplitude $\Delta A = A_x - A_y$ normalised to the total $\tilde{S} = HH + HV + VV + VH$ transmission spectrum (a) and retardance phase $\Delta\psi = \psi_x - \psi_y$ (b) calculated from the best fit by Eq. 1. The inset in (a) shows color conventions for input polarisation.

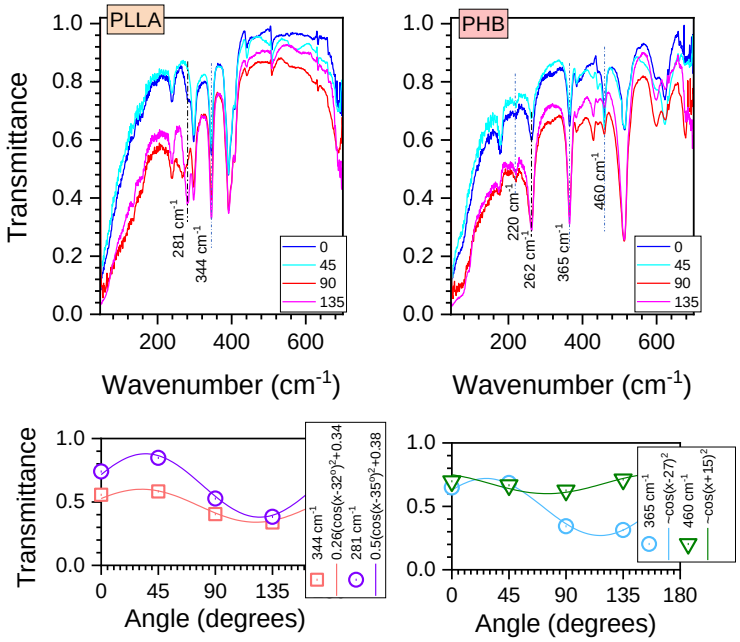

Fig. S4 (Top) Transmittance T spectra (in ATR mode) at four fixed input orientation angles at IN-port $\theta_{IN} = 0, \pi/4, \pi/2, 3\pi/4$, observed for PLLA (left) and PHB (right). Transmittance at the OUT-port was calculated as a sum at two orthogonal polarisations using (IN,OUT) convention: $T(\theta_{IN}; \theta_{sum}) = \theta H + \theta V$. (Bottom) The 4-angle polarisation fit at selected absorption bands (at a single wavenumber). Fits were made using $f(\theta) = a\cos^2(\theta - \theta_A) + \text{Offset}$, where θ_A is the angle of maximum absorbance (dipole orientation).